

Modeling Non-Heme Iron Halogenases: High-Spin Oxoiron(IV)–Halide Complexes That Halogenate C–H Bonds

Mayank Puri,[†] Achintesh N. Biswas,[†] Ruixi Fan,[‡] Yisong Guo,^{*,‡} and Lawrence Que, Jr.^{*,†}

[†]Department of Chemistry and Center for Metals in Biocatalysis, University of Minnesota, Minneapolis, Minnesota 55455, United States

[‡]Department of Chemistry, Carnegie Mellon University, Pittsburgh, Pennsylvania 15213, United States

S Supporting Information

ABSTRACT: The non-heme iron halogenases CytC3 and SyrB2 catalyze C–H bond halogenation in the biosynthesis of some natural products via $S = 2$ oxoiron(IV)–halide intermediates. These oxidants abstract a hydrogen atom from a substrate C–H bond to generate an alkyl radical that reacts with the bound halide to form a C–X bond chemoselectively. The origin of this selectivity has been explored in biological systems but has not yet been investigated with synthetic models. Here we report the characterization of $S = 2$ $[\text{Fe}^{\text{IV}}(\text{O})(\text{TQA})(\text{Cl}/\text{Br})]^+$ (TQA = tris(quinolyl-2-methyl)amine) complexes that can preferentially halogenate cyclohexane. These are the first synthetic oxoiron(IV)–halide complexes that serve as spectroscopic and functional models for the halogenase intermediates. Interestingly, the nascent substrate radicals generated by these synthetic complexes are not as short-lived as those obtained from heme-based oxidants and can be intercepted by O_2 to prevent halogenation, supporting an emerging notion that rapid rebound may not necessarily occur in non-heme oxoiron(IV) oxidations.

Non-heme iron halogenases are an important subset of the family of αKG -dependent non-heme iron enzymes that utilize O_2 to halogenate substrate C–H bonds in the biosynthesis of some natural products.¹ Two well-studied examples are CytC3 and SyrB2, the enzymes responsible for the synthesis of cytrotienin A/B and syringomycin E, which have antitumor and biosurfactant properties, respectively.^{2,3} The halogenase active site differs from those of other αKG -dependent iron enzymes in having a halide ligand in place of the carboxylate of the canonical 2-His-1-carboxylate facial triad that binds the iron.⁴ Despite this change, the mechanism of dioxygen activation by non-heme iron halogenases is thought to be analogous to that of other αKG -dependent non-heme iron enzymes. The active oxidant derived therefrom is proposed to be an $S = 2$ oxoiron(IV)–halide species that abstracts a hydrogen atom to form a hydroxoiron(III)–halide species and a substrate radical. In the next step, the incipient radical can undergo rebound with either the hydroxo or halo ligand to afford respective R–OH or R–Cl products. In an elegant study, Matthews et al.⁵ showed that substrate positioning controls the chemoselectivity of halogenation over hydroxylation in SyrB2, which was corroborated by HYSCORE studies of SyrB2–substrate–NO complexes.⁶

There has been some effort to obtain synthetic models for the oxoiron(IV)–halide intermediates of the halogenases. Notable examples are $\text{Fe}^{\text{IV}}(\text{O})(\text{L})(\text{Cl}/\text{Br})$ complexes, where L = tris(pyridyl-2-methyl)amine (TPA),⁷ 1-(pyridyl-2-methyl)-4,7-dimethyl-1,4,7-triazacyclononane (PyTACN),⁸ or *N*-methyl-1,1-bis{2-[*N*²-(1,1,3,3-tetramethylguanidino)]ethyl}amine (TMG₂dien),⁹ obtained by halide exchange with the bound solvent of the $\text{Fe}^{\text{IV}}(\text{O})(\text{L})(\text{solvent})$ precursor. The first two have $S = 1$ spin states, while the third has an $S = 2$ spin state (Tables 1 and S1).¹⁰ While these complexes serve as suitable spectroscopic models, no oxoiron(IV)–halide complex has yet been demonstrated to transform C–H bonds into C–(Cl/Br) bonds. Some iron complexes capable of oxidative ligand transfer are known, but the actual oxidants in these systems have not been identified.^{11–13} Here we report synthetic complexes that serve as spectroscopic and functional models for the $S = 2$ oxoiron(IV)–halide intermediates of non-heme iron halogenases.

We recently reported the generation of an $S = 2$ oxoiron(IV) complex, $[\text{Fe}^{\text{IV}}(\text{O})(\text{TQA})(\text{MeCN})]^{2+}$ (**1**) (TQA = tris(quinolyl-2-methyl)amine), that serves as both a spectroscopic and functional model of TauD-*J*, the oxoiron(IV) intermediate of the non-heme iron enzyme taurine dioxygenase that effects taurine hydroxylation (Table 1).¹⁴ Addition of 1 equiv of NBu_4X (X = Cl, Br) to **1** in MeCN at -40°C initiates ligand exchange to afford the oxoiron(IV) complexes $[\text{Fe}^{\text{IV}}(\text{O})(\text{TQA})(\text{Cl})]^+$ (**2**) and $[\text{Fe}^{\text{IV}}(\text{O})(\text{TQA})(\text{Br})]^+$ (**3**), respectively (Figure 1). UV–vis titration experiments (Figure S1) show that 1 equiv of halide is sufficient to generate these new species fully. Complexes **2** and **3** are less stable than **1**, with half-lives at -40°C of approximately 5 min, corresponding to 3-fold faster self-decay.

The electronic spectra of **2** and **3** display features at 370 nm ($\epsilon \approx 5000 \text{ M}^{-1} \text{ cm}^{-1}$), 625 nm ($\epsilon = 460 \text{ M}^{-1} \text{ cm}^{-1}$), and 875 nm ($\epsilon = 110 \text{ M}^{-1} \text{ cm}^{-1}$), which are blue-shifted relative to those of **1** (Figure 1). A small blue shift was also seen when MeCN in the $S = 2$ complex $[\text{Fe}^{\text{IV}}(\text{O})(\text{TMG}_2\text{dien})(\text{MeCN})]^{2+}$ (**6**) was replaced with chloride (**7**).⁹ In contrast, $S = 1$ $[\text{Fe}^{\text{IV}}(\text{O})(\text{L})(\text{MeCN})]^{2+}$ complexes with L = TPA⁷ or PyTACN⁸ exhibit near-IR features that are red-shifted by 50–80 nm upon halide addition (Table 1), which can be rationalized by the fact that halide anions are weaker-field ligands than MeCN. An explanation for the observed blue shifts in going from **1** to **2** and **3** will require a better understanding of the electronic spectra of this new family of $S = 2$ oxoiron(IV) complexes.

Received: November 9, 2015

Published: February 15, 2016



Table 1. Spectroscopic Properties of $S = 2$ $\text{Fe}^{\text{IV}}=\text{O}$ Species

| complex | λ_{max} (nm) | δ (mm/s) | ΔE_{O} (mm/s) | $\nu(\text{Fe}=\text{O})$ (cm^{-1}) | ref |
|-----------------------|-----------------------------|-----------------|------------------------------|--|-------|
| 1 | 380 (br), 650, 900 | 0.24 | -1.05 | 838 (-35) | 14 |
| 2 | 370 (br), 625, 875 | 0.22 | 0.96 ^b | 827 (-35) | a |
| 3 | 370 (br), 625, 875 | 0.21 | 0.94 ^b | 828 (-37) | a |
| 6 | 380, 805 | 0.08 | 0.58 | 807 (-34) | 9 |
| 7 | 385, 803, 825 | 0.08 | 0.41 | 810 (-35) | 9 |
| TauD-J | 318 | 0.30 | -0.90 | 821 (-34) | 17 |
| SyrB2-Cl ^c | 318 | 0.23 | 0.76 ^b | 824 ^d | 3, 15 |
| | | 0.30 | 1.09 ^b | | |
| CytC3-Cl | 318 | 0.22 | -0.70 | | 2a |
| | | 0.30 | -1.09 | | |
| CytC3-Br | | 0.23 | -0.81 | | 2b |
| | | 0.31 | -1.06 | | |

^aThis work. ^bThe sign of ΔE_{O} was not determined. ^cThe experimental values were obtained from the reaction of SyrB2 with L-Thr-S-SyrB1. ^dObtained from DFT calculations (ref 15).

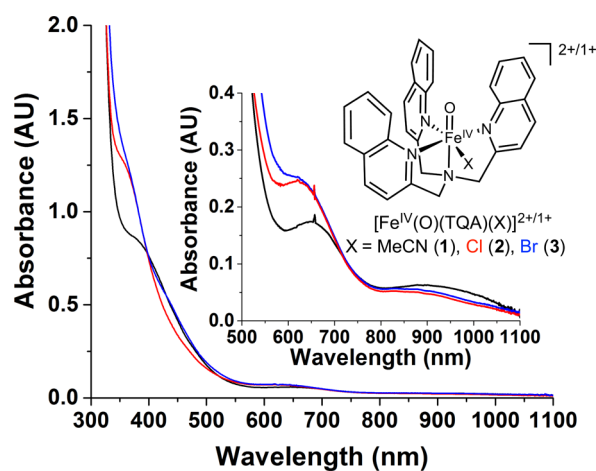


Figure 1. UV-vis spectra of 0.25 mM solutions of 1 (black), 2 (red), and 3 (blue) in MeCN at -40 °C. Inset: spectra of 1.0 mM solutions of 1 (black), 2 (red), and 3 (blue) focused on the near-IR region.

Evidence that the $\text{Fe}=\text{O}$ unit is retained in 2 and 3 is provided by resonance Raman spectroscopy. Excitation of frozen solutions of 2 and 3 at 514.5 nm reveals bands at 827 and 828 cm^{-1} , respectively (Figures S2a and S3a), representing downshifts of ~ 10 cm^{-1} relative to that of 1. ^{18}O labeling of 2 and 3 elicits respective downshifts of 35 and 37 cm^{-1} (Figures S2b and S3b), consistent with the 36 cm^{-1} shift calculated for an $\text{Fe}=\text{O}$ vibration by Hooke's law. These values nearly match the frequencies predicted by DFT for the $\text{Fe}^{\text{IV}}(\text{O})\text{Cl}$ and $\text{Fe}^{\text{IV}}(\text{O})\text{Br}$ intermediates of SyrB2 (824 and 825 cm^{-1}).¹⁵

Mössbauer analysis of 2 and 3 at 4.2 K shows quadrupole doublets for the oxoiron(IV) centers, representing 65% and 70% of the iron in the samples, respectively, with parameters similar to those of 1¹⁴ (Table 1 and Figures S4 and S5). Monoferric and diferric byproducts make up the balance of the iron in the samples. Complexes 2 and 3 exhibit isomer shifts of 0.22 and 0.21 mm/s, respectively, which are within the range found for non-heme enzyme intermediates with $S = 2$ oxoiron(IV) centers (Tables 1 and S2). Other synthetic $S = 2$ oxoiron(IV) centers have isomer shifts out of this range, namely, 0.38 mm/s for the $[\text{Fe}^{\text{IV}}(\text{O})(\text{OH}_2)_5]^{2+}$ ion characterized by Bakac^{16a} and ≤ 0.10

mm/s for the trigonal-bipyramidal oxoiron(IV) complexes described by Borovik,^{16b} Chang,^{16c} and Que^{16d} (Tables 1 and S1). Interestingly, the oxoiron(IV)-halide intermediates of CytC3 and SyrB2 exhibit two quadrupole doublets with distinct isomer shifts, one at 0.30 mm/s matching that of the prototypical TauD-J enzyme intermediate and the other at 0.23 mm/s, which is close to the values for 2 and 3 (Tables 1 and S2). As has been pointed out, TQA is the only polydentate ligand to date that serves as a good electronic mimic for the iron coordination environments of TauD, CytC3, and SyrB2.¹⁰

DFT calculations on 2 and 3 were performed to obtain geometry-optimized structures, and the calculated Mössbauer isomer shifts match the experimental values. These afford $\text{Fe}=\text{O}$ distances of 1.64 Å for both 2 and 3 and $\text{Fe}-\text{Cl}$ and $\text{Fe}-\text{Br}$ distances of 2.36 and 2.51 Å, respectively (Figure 2 and Table

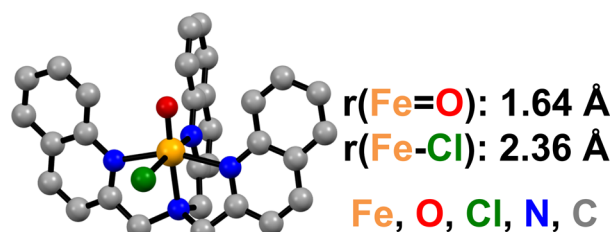


Figure 2. DFT-calculated structure of 2.

S3). The latter distances are consistent with the EXAFS-derived distances of 2.31 and 2.43 Å measured for the oxoiron(IV)-halide intermediates of SyrB2-Cl and CytC3-Br, respectively.^{2b,3}

Previously, we noted that 1 is the most reactive synthetic non-heme oxoiron(IV) complex reported to date, as it can cleave the C-H bonds of cyclohexane at -40 °C at a rate approaching that for substrate C-H bond cleavage by TauD-J at 5 °C after adjustment for temperature, producing a 35% yield of cyclohexanone.¹⁴ In extending our reactivity study to 2 and 3, we found that their reactions with cyclohexane at -40 °C afforded halocyclohexanes, cyclohexanol, and cyclohexanone, as identified by ^1H NMR spectroscopy (Figures S9-S13). The halogenated products were obtained in 3-6-fold higher yields than the oxygenated products (Table 2). With toluene as the substrate,

Table 2. Product Yields for the Reactions of 1-3 with Cyclohexane and Toluene under N_2 in CD_3CN at -40 °C^a

| product | cyclohexane | | | toluene | | |
|---------|----------------|-----|-----|---------|-----|-----|
| | 1 ^b | 2 | 3 | 1 | 2 | 3 |
| R-X | — | 35% | 41% | 2% | 25% | 33% |
| R-OH | — | 7% | 3% | 27% | 13% | 7% |
| R=O | 35% | 3% | 4% | 15% | 19% | 22% |

^aFor details, see p S12 in the Supporting Information. ^bFrom ref 14.

more comparable yields of halogenated and oxygenated products were observed. These results represent the first examples of substrate halogenation by a bona fide synthetic $S = 2$ $\text{Fe}^{\text{IV}}(\text{O})(\text{X})$ complex, thereby mimicking the reactivity of the oxoiron(IV)-halide intermediates of SyrB2 and CytC3.

To gain more insight into the halogenation reactions, kinetic studies were carried out on 2 and 3. For cyclohexane oxidation, 2 and 3 decayed at rates comparable to the self-decay rate, so second-order rate constants could not be determined. On the other hand, toluene was oxidized at significantly higher rates because of its weaker aliphatic C-H bonds. Kinetic analysis

showed that 2 and 3 react with toluene at rates approximately 10-fold smaller than that for 1 (Figures 3, S7, and S8), reflecting the

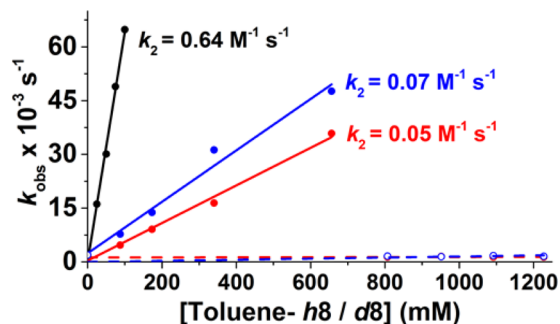


Figure 3. Plots of pseudo-first-order rate constants (k_{obs}) vs the concentration of toluene- h_8 (solid lines) or toluene- d_8 (dashed lines) for 1 (black), 2 (red), and 3 (blue).

trend of decreased substrate C–H bond cleavage rates observed for the oxoiron(IV) intermediates of the halogenases SyrB2 and CytC3 versus TauD-J.⁵ Interestingly, this reactivity trend is opposite to that for the $S = 1$ $[\text{Fe}^{\text{IV}}(\text{O})(\text{PyTACN})(\text{X})]^+$ complexes, where the halo variants oxidize 9,10-dihydroanthracene (DHA) 2–3-fold faster than the parent MeCN complex does.⁸ With these results in mind, there are four important mechanistic points to clarify about the observed halogenation: (a) the nature of the species that cleaves the substrate C–H bond, (b) whether the classic fast-rebound mechanism applies to 2 and 3, (c) the role of the iron(IV) spin state, and (d) the chemoselectivity between hydroxylation and halogenation.

To ascertain whether the $\text{Fe}=\text{O}$ unit in 2 and 3 is responsible for the initial C–H bond cleavage, we measured the kinetic isotope effect with toluene as the substrate. As shown in Figure 3, the oxidation of toluene- h_8 by 2 and 3 is significantly faster than that of toluene- d_8 , which occurs at a rate comparable to that of the self-decay (Figure 3, dashed blue and red lines). These results show that C–H bond cleavage by the oxoiron(IV) species 2 and 3 must be the rate-determining step, with a KIE well above the classical limit of 7. Other non-heme oxoiron(IV) complexes have been found to exhibit large nonclassical KIEs, implicating a significant contribution from a tunneling mechanism for H-atom abstraction.^{14,18} A more accurate estimate of the KIE could be obtained from the benzyl bromide- h_7/d_7 product ratio for the intermolecular competitive halogenation of toluene- h_8 and toluene- d_8 by 3. A value of 20 was obtained (for experimental details, see p S13 and Figure S14 in the Supporting Information), which is comparable to the KIE of 25 reported for the oxidation of toluene by 1.¹⁴ The observed large KIE also excludes the possibility of free radical bromination of toluene, for which a much smaller KIE value of 4.9 has been reported in such a reaction with toluene- $\alpha-d_2$;¹⁹ furthermore, the yield of R–Br did not increase with the addition of excess bromide ion and in fact decreased by 30% with 5–20 equiv of added bromide ion (Table S4). Even more importantly, the toluene KIE value we measured for 3 is essentially identical to that reported by Matthews et al.³ for oxidation of the C4-protio and C4-deuterio native substrate in SyrB2. Taken together, these data support the notion that the initial C–H bond cleavage step occurs via H-atom abstraction by the oxoiron(IV)–halide complexes 2 and 3.

H-atom abstraction from the substrate should initially convert 2 and 3 into hydroxoiron(III)–halide species together with an organic radical within a solvent cage (Figure 4). If the P450



Figure 4. Proposed mechanisms for substrate hydroxylation and halogenation by 2–5.

paradigm applies to this chemistry,²⁰ the alkyl radical would then react with the incipient $\text{Fe}^{\text{III}}(\text{OH})(\text{X})$ species in a rapid rebound step to yield hydroxylated or halogenated products. Alternatively, the radical may be longer lived than those found in heme systems and escape from the solvent cage to react with other species in solution,²¹ such as residual $\text{Fe}^{\text{IV}}(\text{O})(\text{X})$ or radical traps such as O_2 . The latter mechanistic outcome has been demonstrated experimentally by Nam in studies of several $S = 1$ non-heme oxoiron(IV) complexes.²²

To assess the lifetime of the nascent substrate alkyl radical produced in the reactions of 2 and 3, O_2 was introduced into the reaction mixture to act as a radical trap (Figure 4), giving rise to no halogenation and exclusive formation of oxygenated products (Tables 3 and S5). These results show that C–X bond formation

Table 3. Product Yields (vs Fe(II) Precursors) for the Reactions of 2, 3, $[\text{Fe}^{\text{IV}}(\text{O})(\text{TPA})(\text{Cl})]^+$ (4), and $[\text{Fe}^{\text{IV}}(\text{O})(\text{TPA})(\text{Br})]^+$ (5) with Cyclohexane in CD_3CN

| product | $S = 2$ TQA (-40°C) | | $S = 1$ TPA (25°C) | |
|---------|-------------------------------------|--------------|------------------------------------|--------------|
| | N_2 | O_2 | N_2 | O_2 |
| R–Cl | 35% | 0% | 11% | 0% |
| R–OH | 7% | 22% | 0% | 12% |
| R=O | 3% | 39% | 2% | 4% |
| R–Br | 41% | 0% | 13% | 0% |
| R–OH | 3% | 8% | 0% | 6% |
| R=O | 4% | 24% | 2% | 3% |

with the alkyl radical is not as fast as its interception by O_2 ,^{23,24} unlike the case of heme-based systems.²⁰ Thus, the observed halogenation in the absence of O_2 likely occurs by a relatively slow radical recombination step with either the $\text{Fe}^{\text{III}}(\text{OH})(\text{X})$ species within the solvent cage or remaining $\text{Fe}^{\text{IV}}(\text{O})(\text{X})$ species following cage escape. Either scenario can account for the ferric decay products observed in the Mössbauer spectra of frozen solutions of 3 after reaction with substrate (Figure S6), as the ferrous byproducts expected from the first scenario readily disproportionate with 2 and 3. The yields of halogenated products are consistent with this explanation, but it is not as clear whether the oxygenated products arise from the same mechanism. These observations concur with recent results of Nam, who has raised questions about the applicability of the heme paradigm to high-valent non-heme metal–oxo species.²² However, both of these results are at odds with a recent report by Maiti providing ESI-MS evidence for oxygen rebound in the reactions of an electron-rich $S = 1$ oxoiron(IV) complex.²⁵ Clearly, more effort is required in order to clarify the factors that control the rate of rebound in synthetic non-heme iron systems.

To assess the role that the spin state may play in C–H bond halogenation, the oxidation of cyclohexane was tested with the $S = 1$ complexes $[\text{Fe}^{\text{IV}}(\text{O})(\text{TPA})(\text{Cl})]^+$ (4) and $[\text{Fe}^{\text{IV}}(\text{O})(\text{TPA})(\text{Br})]^+$ (5) under the same conditions, except for a change in temperature to 25°C to compensate for their lack of reactivity at -40°C . These reactions showed the selective formation of halocyclohexane, albeit in lower yields than with 2 and 3 (Table 3), indicating that the $S = 2$ spin state is not an absolute

requirement for halogenation. Experiments with **4** and **5** under O₂ also resulted in complete loss of halogenation, suggesting that C–X bond formation is slower than radical interception by O₂ as well for S = 1 non-heme oxoiron(IV) complexes.

Finally, our results also shed some light on the chemoselectivity of C–X bond formation in the absence of a protein scaffold. Table 3 shows halogenation to be favored over hydroxylation in cyclohexane oxidation by all four complexes studied. These results suggest that oxidative ligand transfer may be influenced by electronic factors such as the oxidizability of the ligand, as Cl[–] and Br[–] have lower oxidation potentials (1.36 and 1.07 V, respectively) versus OH[–] (2.02 V).²⁶ Steric factors seem less likely to play a role, as both TPA and TQA complexes favor halogenation despite the larger steric bulk of the quinoline donors. Clearly, additional synthetic examples are needed to establish whether this is a general trend and to rationalize the decreased chemoselectivity observed in the oxidation of toluene by **2** and **3**. In contrast, the chemoselectivity of C–H bond functionalization in SyrB2 has been shown to be determined by the positioning of the organic substrate within the active site relative to the nascent oxoiron(IV)–halide oxidant.⁵

In summary, we have reported the first examples of C–H bond halogenation by synthetic oxoiron(IV)–halide complexes. Although halogenation products are observed irrespective of the spin state of the oxoiron(IV) unit, the S = 2 complexes **2** and **3** are more effective halogenation agents and react much more rapidly. Moreover, they are the only synthetic complexes to reproduce the Mössbauer parameters of the S = 2 oxoiron(IV) intermediates of the halogenases.^{3,5} Thus, **2** and **3** are excellent spectroscopic and functional models of the CytC3 and SyrB2 intermediates and support nature's choice of the S = 2 spin state for the oxoiron(IV) oxidants in the halogenases. These complexes may also serve as models for the yet unobserved oxidants associated with the iron-catalyzed halogenations reported by Comba¹¹ and Paine.¹² Finally, our studies suggest that C–X bond formation by **2**–**5** is not as rapid as C–O bond formation in heme-mediated C–H bond oxidations,²⁰ in agreement with results reported by Nam on S = 1 non-heme oxoiron(IV) complexes.²² These results raise the intriguing question of whether the classic oxygen rebound mechanism applies to the high-valent metal centers in mononuclear non-heme iron oxygenases. To the best of our knowledge, there is no unequivocal stereochemical evidence to date that requires fast rebound in the catalytic cycles of these enzymes.

■ ASSOCIATED CONTENT

Supporting Information

The Supporting Information is available free of charge on the ACS Publications website at DOI: 10.1021/jacs.5b11511.

Experimental details and additional data (PDF)

■ AUTHOR INFORMATION

Corresponding Authors

*larryque@umn.edu

*ysguo@andrew.cmu.edu

Notes

The authors declare no competing financial interest.

■ ACKNOWLEDGMENTS

We thank NSF for funding (CHE-1361773 to L.Q.), the University of Minnesota for a doctoral dissertation fellowship to M.P., the Indo–U.S. Science & Technology Forum for a

postdoctoral fellowship to A.N.B., and Ms. Jale Ocal for results on cyclohexane oxidation by [Fe^{IV}(O)(TPA)(MeCN)]²⁺.

■ REFERENCES

- (1) (a) Krebs, C.; Fujimori, D. G.; Walsh, C. T.; Bollinger, J. M., Jr. *Acc. Chem. Res.* **2007**, *40*, 484. (b) Bollinger, J. M., Jr.; Chang, W.-C.; Matthews, M. L.; Martinie, R. J.; Boal, A. K.; Krebs, C. In *2-Oxoglutarate-Dependent Oxygenases*; Hausinger, R. P., Schofield, C. J., Eds.; Royal Society of Chemistry: Cambridge, U.K., 2015; pp 95–122.
- (2) (a) Galonić, D. P.; Barr, E. W.; Walsh, C. T.; Bollinger, J. M., Jr.; Krebs, C. *Nat. Chem. Biol.* **2007**, *3*, 113. (b) Galonić, D. P.; Barr, E. W.; Matthews, M. L.; Koch, G. M.; Yonce, J. R.; Walsh, C. T.; Bollinger, J. M., Jr.; Krebs, C.; Riggs-Gelasco, P. J. *J. Am. Chem. Soc.* **2007**, *129*, 13408.
- (3) Matthews, M. L.; Krest, C. M.; Barr, E. W.; Vaillancourt, F. H.; Walsh, C. T.; Green, M. T.; Krebs, C.; Bollinger, J. M., Jr. *Biochemistry* **2009**, *48*, 4331.
- (4) Blasiak, L. C.; Vaillancourt, F. H.; Walsh, C. T.; Drennan, C. L. *Nature* **2006**, *440*, 368.
- (5) Matthews, M. L.; Neumann, C. S.; Miles, L. A.; Grove, T. L.; Booker, S. J.; Krebs, C.; Walsh, C. T.; Bollinger, J. M., Jr. *Proc. Natl. Acad. Sci. U. S. A.* **2009**, *106*, 17723.
- (6) Martinie, R. J.; Livada, J.; Chang, W.-C.; Green, M. T.; Krebs, C.; Bollinger, J. M.; Silakov, A. *J. Am. Chem. Soc.* **2015**, *137*, 6912.
- (7) Rohde, J.-U.; Stubna, A.; Bominaar, E. L.; Münck, E.; Nam, W.; Que, L., Jr. *Inorg. Chem.* **2006**, *45*, 6435.
- (8) Planas, O.; Clemancey, M.; Latour, J.-M.; Company, A.; Costas, M. *Chem. Commun.* **2014**, *50*, 10887.
- (9) England, J.; Guo, Y.; Van Heuvelen, K. M.; Cranswick, M. A.; Rohde, G. T.; Bominaar, E. L.; Münck, E.; Que, L., Jr. *J. Am. Chem. Soc.* **2011**, *133*, 11880.
- (10) Puri, M.; Que, L. *Acc. Chem. Res.* **2015**, *48*, 2443.
- (11) Comba, P.; Wunderlich, S. *Chem. - Eur. J.* **2010**, *16*, 7293.
- (12) Chatterjee, S.; Paine, T. K. *Angew. Chem., Int. Ed.* **2016**, DOI: 10.1002/anie.201509914.
- (13) Sharma, A.; Hartwig, J. F. *Nature* **2015**, *517*, 600.
- (14) Biswas, A. N.; Puri, M.; Meier, K. K.; Oloo, W. N.; Rohde, G. T.; Bominaar, E. L.; Münck, E.; Que, L. *J. Am. Chem. Soc.* **2015**, *137*, 2428.
- (15) Wong, S. D.; Srncic, M.; Matthews, M. L.; Liu, L. V.; Kwak, Y.; Park, K.; Bell, C. B., III; Alp, E. E.; Zhao, J.; Yoda, Y.; Kitao, S.; Seto, M.; Krebs, C.; Bollinger, J. M., Jr.; Solomon, E. I. *Nature* **2013**, *499*, 320.
- (16) (a) Pestovsky, O.; Stoian, S.; Bominaar, E. L.; Shan, X.; Münck, E.; Que, L., Jr.; Bakac, A. *Angew. Chem., Int. Ed.* **2005**, *44*, 6871. (b) Lacy, D. C.; Gupta, R.; Stone, K. L.; Greaves, J.; Ziller, J. W.; Hendrich, M. P.; Borovik, A. S. *J. Am. Chem. Soc.* **2010**, *132*, 12188. (c) Bigi, J. P.; Harman, W. H.; Lassalle-Kaiser, B.; Robles, D. M.; Stich, T. A.; Yano, J.; Britt, R. D.; Chang, C. J. *J. Am. Chem. Soc.* **2012**, *134*, 1536. (d) England, J.; Martinho, M.; Farquhar, E. R.; Frisch, J. R.; Bominaar, E. L.; Münck, E.; Que, L., Jr. *Angew. Chem., Int. Ed.* **2009**, *48*, 3622.
- (17) (a) Sinnecker, S.; Svendsen, N.; Barr, E. W.; Ye, S.; Bollinger, J. M., Jr.; Neese, F.; Krebs, C. *J. Am. Chem. Soc.* **2007**, *129*, 6168. (b) Proshlyakov, D. A.; Henshaw, T. F.; Monterosso, G. R.; Ryle, M. J.; Hausinger, R. P. *J. Am. Chem. Soc.* **2004**, *126*, 1022.
- (18) Kleespies, S. T.; Oloo, W. N.; Mukherjee, A.; Que, L. *Inorg. Chem.* **2015**, *54*, 5053.
- (19) Wiberg, K. B. *Chem. Rev.* **1955**, *55*, 713.
- (20) Groves, J. T. *J. Chem. Educ.* **1985**, *62*, 928.
- (21) Barton, D. H. R.; Doller, D. *Acc. Chem. Res.* **1992**, *25*, 504.
- (22) (a) Cho, K.-B.; Wu, X.; Lee, Y.-M.; Kwon, Y. H.; Shaik, S.; Nam, W. *J. Am. Chem. Soc.* **2012**, *134*, 20222. (b) Cho, K.-B.; Hirao, H.; Shaik, S.; Nam, W. *Chem. Soc. Rev.* **2016**, DOI: 10.1039/C5CS00566C.
- (23) Achord, J. M.; Hussey, C. L. *Anal. Chem.* **1980**, *52*, 601–602.
- (24) Wu, D.; Bayes, K. D. *Int. J. Chem. Kinet.* **1986**, *18*, 547.
- (25) Rana, S.; Dey, A.; Maiti, D. *Chem. Commun.* **2015**, *51*, 14469.
- (26) *CRC Handbook of Chemistry and Physics*, 77th ed.; Lide, D. R., Ed.; CRC Press: Boca Raton, FL, 1996; pp 8–20.